Li+/Na+ β-Alumina: A Combined Single-Crystal Neutron and X-ray Diffraction Study

Kristina Edström,[a] Torbjörn Gustafsson,[a]* John O. Thomas[a] and Gregory C. Farrington[b]

[a]*Department of Inorganic Chemistry, Ångström Laboratory, University of Uppsala, Box 538, S-751 21 Uppsala, Sweden, and* [b]*Department of Materials Science and Engineering, University of Pennsylvania, Philadelphia, PA 19104, USA. E-mail: torbjorn.gustafsson@kemi.uu.se*

Abstract

The crystal structure and ionic distribution in the conduction plane of the partially exchanged Na+ β-alumina system $Li_{0.75}Na_{0.47}Al_{11}O_{17.11}$ has been determined from single-crystal X-ray diffraction at 30 and 298 K, in combination with a single-crystal neutron diffraction study at 295 K. At 30 K the Li+ ions occupy two sites: one in (2/3, 1/3, 1/4) and one ~1.0 Å out of the $z = 1/4$ conduction plane. The Na+ ions are also found in two sites, both in the conduction plane. At 298 K the Li+ ions are found in three sites; the same two sites as at 30 K, as well as at a third site between these two. The Na+ ions occupy the same sites as at 30 K. The combination of X-ray and neutron diffraction is used to resolve the distribution of Na+ and Li+ ions. The column O5 atom in the Al3—O5—Al3 bridge between the spinel blocks is found to be disordered. Charge compensation is achieved through a Frenkel defect of two interstitial Al atoms, one on either side of the conduction plane, together with an extra oxygen in the conduction plane. One such defect occurs, on average, in every 4.5 unit cells.

1. Introduction

It is of technological interest to find solid Li+ ion conductors with conductivities high enough for battery applications. Although Li+ β-alumina is difficult to prepare as a single phase and free from water, it is nevertheless one of the best solid Li+ ion conductors: $\sigma \simeq 3 \times 10^{-3}\ \Omega^{-1}\ cm^{-1}$ at 298 K (Briant & Farrington, 1981) compared with $4.1 \times 10^{-6}\ \Omega^{-1}\ cm^{-1}$ for $Li_{0.8}Zr_{1.8}Ta_{0.2}P_3O_{12}$ at 298 K (Shannon, Taylor, English & Berzins, 1977) and $2 \times 10^{-6}\ \Omega^{-1}\ cm^{-1}$ for LISICON (solid solutions based on stoichiometric phases such as γ-Li_2ZnGeO_4) at 323 K (von Alpen, Bell & Wichelhaus, 1978). Its structure consists of rigid spinel blocks of aluminium oxide interleaved by conduction layers containing the Li+ ions (Fig. 1). Li+ β-alumina is prepared from Na+ β-alumina by ion exchange in a molten lithium salt mixture. Na+ β-alumina, $Na_{1.22}Al_{11}O_{17.11}$, is an excellent Na+-ion conductor and has, as such, been used as solid electrolyte in the Na/S battery. The Na+ ions can easily be exchanged for other, monovalent and, in some cases divalent, cations (Yao & Kummer, 1967;

Sutter, Cratty, Saltzberg & Farrington, 1983). This has facilitated the synthesis of a whole range of compounds, of which Li+ β-alumina is one example. A wide range of experimental values for Li+ ion conductivity has been quoted (Briant & Farrington, 1981), all for samples
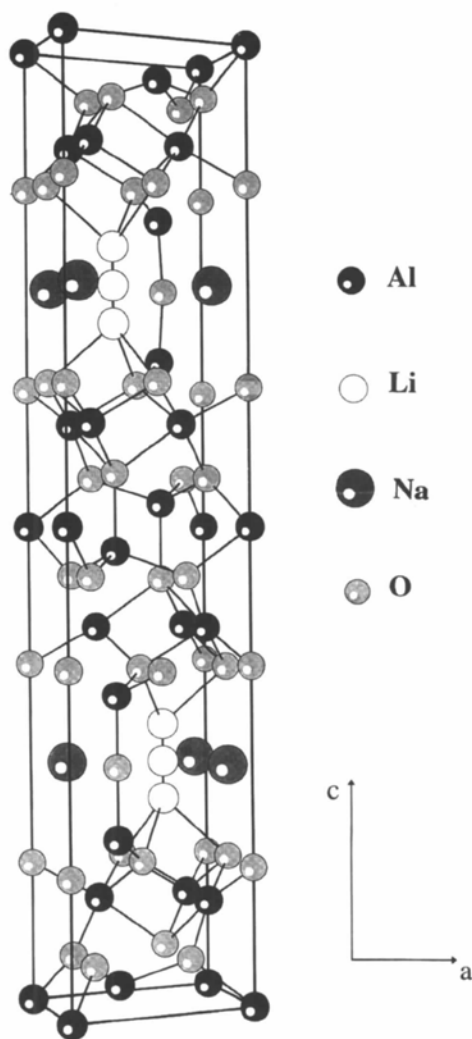

Fig. 1. The unit cell of Li+/Na+ β-alumina. The figure was produced with the program *Moviemol* (Hermansson & Ojamae, 1993).

prepared by ion exchange. As discussed by Briant & Farrington (1981), these variations could well be a result of variable amounts of residual Na$^+$ ions.

Two earlier structural studies of a Li$^+$ β-alumina system have been reported: a powder neutron diffraction study of Li$^+$/Na$^+$ β-alumina (Tofield & Farrington, 1979), in which the Li$^+$ ions were found outside the conduction plane on either side of the mid-oxygen (mO) site. A single-crystal study of hydrated Li$^+$ β-alumina has also appeared: no Li$^+$ ion distribution was given, but the possibility of the Li$^+$ ions lying outside the $z = 1/4$ mirror plane was discussed (Dudney *et al.*, 1981; Bates, Dudney, Brown, Wang & Frech, 1982). There is also a Raman study of Li$^+$ β-alumina, where the Li$^+$ ions were found to occupy both Beevers–Ross (BR) sites (Beevers & Ross, 1937) and sites $\sim$0.8 Å from the BR site in the conduction plane (Kaneda, Bates & Wang, 1978). A positive pressure coefficient of resistivity has also been observed (Radzilowski & Kummer, 1971), which can suggest a Li$^+$ ion displacement off the mirror plane.

A combined X-ray and neutron diffraction study has been undertaken here on the same single crystal of Li$^+$/Na$^+$ β-alumina. The X-ray study was made at both 30 and 298 K to distinguish mixed-ion distribution from thermal effects. A further aim of this study is to relate the distribution of the Li$^+$ and Na$^+$ ions to a possible conductivity mechanism for the Li$^+$ ions. The results will be compared to the structure of Na$^+$ β-alumina and discussed in light of the Na$^+$ ion conductivity mechanism. An explanation as to why it is difficult to obtain fully exchanged Li$^+$ β-alumina is also sought.

2. Experimental

A cut single crystal of Na$^+$ β-alumina (Union Carbide) of the dimensions 2.25 × 4.45 × 0.55 mm was used as a starting material. Li$^+$ β-alumina was prepared by ion exchange of the Na$^+$ β-alumina crystal in molten LiCl at 948 K. While full exchange of sodium for lithium was earlier assumed, the X-ray and neutron diffraction studies here indicate only partial Na$^+$ ion exchange and a composition of Li$_{0.75}$Na$_{0.47}$Al$_{11}$O$_{17.11}$. Although several efforts were made with different chemical analysis techniques (*e.g.* X-ray fluorescence and absorption spectroscopy), the amount of compound present did not allow for a chemical analysis, since it was needed for the diffraction experiment.

Neutron diffraction data were collected at the R2 medium flux reactor at Studsvik, Sweden. Experimental details given in Table 1.

X-ray diffraction data sets at two different temperatures, 30 and 298 K, were collected on a small single crystal extracted from the large crystal used earlier for the neutron diffraction experiment. The crystal was heat treated for 24 h at $\sim$575 K and then transferred to the diffractometer in a box containing dry air. A

STOE four-circle diffractometer was equipped with a large Huber circle and a two-stage cryostat, which was evacuated to 10^{-7} atm. The crystal was cooled to 30 K and a data set was collected. The temperature was then increased to room temperature, 298 K, and a new data set was collected. Experimental details are given in Table 1. The intensity data for both data sets were corrected for background (Lehman & Larsen, 1974) and five to six standard reflections (Table 1) were used to scale intensities and standard deviations (McCandlish, Stout & Andrews, 1975). Lp and absorption corrections were applied, the latter by numerical integration. Refinements were made using a PC version of the full-matrix least-squares program *DUPALS* (Lundgren, 1982). The function minimized was $\Sigma w(|F_o|^2 - |F_c|^2)^2$, where $w^{-1} = \sigma^2(F_o^2) = \sigma_c^2(F_o^2) + (kF_o^2)^2$; k is an empirical constant set to 0.02 in both X-ray and neutron cases. Isotropic extinction correction were used according to Becker & Coppens (1975). Anomalous dispersion terms and coherent scattering amplitudes as well as neutron scattering lengths for Al^{3+}, O^{2-}, Li$^+$ and Na$^+$ were taken from *International Tables for X-ray Crystallography* (1974). All computer programs were described by Lundgren (1982).

3. Refinement and results

After ion exchange in the LiCl melt, the conduction planes may contain Li$^+$ ions, possible residual Na$^+$ ions and H$_2$O molecules. The compound is hygroscopic and, although the crystals were heat treated and protected, it could not be excluded that some water still remained in the structure. The spinel block does not change significantly during ion exchange: the positional and displacement parameters for the atoms in the spinel block of Na$^+$ β-alumina (Edström, Thomas & Farrington, 1991a) were thus used as starting parameters for the refinements. A model of the ionic distribution was derived from the difference maps of the conduction plane calculated for both X-ray and neutron diffraction data. This model should be consistent both with the observed scattering density in the neutron and X-ray experiments, as well as with the crystal composition.

The first difference map from the neutron diffraction study revealed a negative peak in the BR site (2/3, 1/3, 1/4) and a broad negative band at a site outside the conduction plane (2/3, 1/3, 0.2) on either side of the BR sites. A positive peak was found at the position (0.9, 0.1, 0.25). In the difference maps from the X-ray data set, electron density was found in the same sites as in the neutron diffraction case.

The combined pictures provided by the neutron and X-ray diffraction data indicate that the Li$^+$ ions occupy the BR site and a site at (2/3, 1/3, $\sim$0.2). The remaining positive peak at (0.9, 0.1, 0.25) in the difference maps from the neutron diffraction could be due to residual Na$^+$

Table 1. *Experimental details*

	X-ray, 30 K	Neutron, 295 K	X-ray, 298 K
Crystal data			
Chemical formula	$Li_{0.75}Na_{0.47}Al_{11}O_{17.11}$	$Li_{0.75}Na_{0.47}Al_{11}O_{17.11}$	$Li_{0.75}Na_{0.47}Al_{11}O_{17.11}$
Chemical formula weight	587.18	587.18	587.18
Cell setting	Hexagonal	Hexagonal	Hexagonal
Space group	$P6_3/mmc$	$P6_3/mmc$	$P6_3/mmc$
a (Å)	5.5900 (6)	5.5929 (6)	5.5929 (6)
c (Å)	22.656 (3)	22.652 (3)	22.652 (3)
V (Å^3)	613.11 (8)	613.63 (8)	613.63 (8)
Z	2	2	2
D_x (Mg m^{-3})	3.177	3.177	3.177
Radiation type	Mo $K\alpha$	Neutron	Mo $K\alpha$
Wavelength (Å)	0.71073	1.21	0.71073
No. of reflections for cell parameters	23	23	23
θ range (°)	35–40	35–40	35–40
μ (mm^{-1})	1.02	0.0573	1.02
Temperature (K)	30	295	298
Crystal form	Plate	Plate	Plate
Crystal size (mm)	0.16 × 0.10 × 0.05	4.45 × 2.25 × 0.55	0.16 × 0.10 × 0.05
Crystal color	Transparent	Transparent	Transparent
Data collection			
Diffractometer	Huber–Stoe–ARACOR	ARACOR	Huber–Stoe–ARACOR
Data collection method	$\theta/2\theta$ scans	$\theta/2\theta$ scans	$\theta/2\theta$ scans
Absorption correction	Integration	Integration	Integration
T_{min}	0.8130	0.8890	0.8170
T_{max}	0.9050	0.9690	0.9050
No. of measured reflections	2685	756	2697
No. of independent reflections	1416	379	1406
No. of observed reflections	2480	454	2423
Criterion for observed reflections	$I_{net} > 1\sigma(I_{net})$	$I_{net} > 1\sigma(I_{net})$	$I_{net} > 1\sigma(I_{net})$
R_{int}	0.017	0.036	0.017
θ_{max} (°)	52.49	57.0	52.49
Range of h, k, l	$-1 \rightarrow h \rightarrow 10$	$0 \rightarrow h \rightarrow 6$	$0 \rightarrow h \rightarrow 10$
	$-4 \rightarrow k \rightarrow 10$	$0 \rightarrow k \rightarrow 6$	$-4 \rightarrow k \rightarrow 10$
	$-50 \rightarrow l \rightarrow 38$	$0 \rightarrow l \rightarrow 31$	$-50 \rightarrow l \rightarrow 36$
No. of standard reflections	6	3	5
Frequency of standard reflections (min)	180	180	180
Intensity decay (%)	0.5	1.1	6.2
Refinement			
Refinement on	F^2	F^2	F^2
$R[F^2 > 2\sigma(F^2)]$	0.0363	0.0477	0.0333
$wR(F^2)$	0.0801	0.0684	0.0790
S	2.25	2.59	2.06
No. of reflections used in refinement	2685	756	2697
No. of parameters used	52	38	50
Weighting scheme	$w = 1/[\sigma^2(F^2) + (0.0200F^2)^2]$	$w = 1/[\sigma^2(F^2) + (0.0200F^2)^2]$	$w = 1/[\sigma^2(F^2) + (0.0200F^2)^2]$
$(\Delta/\sigma)_{max}$	0.100	–	0.100
$\Delta\rho_{max}$ (e Å^{-3})	1.103	–	0.923
$\Delta\rho_{min}$ (e Å^{-3})	-0.890	–	-0.560
Extinction method	General isotropic (Becker & Coppens, 1975)	General isotropic (Becker & Coppens, 1975)	Isotropic extinction (Becker & Coppens, 1975)
Extinction coefficient	1086, 41 410	17 117	981
Source of atomic scattering factors	*International Tables for X-ray Crystallography* (1974, Vol. IV)	*International Tables for Crystallography* (1995, Vol. C)	*International Tables for X-ray Crystallography* (1974, Vol. IV)
Computer programs			
Data reduction	*STOEDATR* (Lundgren, 1982)	*ARACOR* (Lundgren, 1982)	*STOEDATR* (Lundgren, 1982)
Structure refinement	*DUPALS* (Lundgren, 1982)	*DUPALS* (Lundgren, 1982)	*DUPALS* (Lundgren, 1982)
Preparation of material for publication	*DISTAN* (Lundgren, 1982)	*DISTAN* (Lundgren, 1982)	*DISTAN* (Lundgren, 1982)

ions; this same site was found to be occupied by sodium in Na$^+$ β-alumina (Edström, Thomas & Farrington, 1991a). The peak could also represent O atoms of a water molecule (Dudney *et al.*, 1981; Bates, Dudney, Brown, Wang & Frech, 1982); no negative peaks were found, however, to represent the associated H atoms. It was concluded that the source of the positive peak was the Na$^+$ ions.

3.1. *Final model*

Further refinement of the X-ray diffraction data located Li$^+$ ions at three different sites: Li1 (0.7, 0.3, 1/4), which is close to the BR site, Li2 (2/3, 1/3, $\sim$0.204) and Li4 (2/3, 1/3, $\sim$0.227) (Fig. 2). If all three sites were refined containing only Li$^+$ ions, considerably more than 1.22 Li$^+$ per formula unit

would result. Some unexchanged Na⁺ ions must still remain in the Na1 site (~0.7, ~0.3, 1/4) and the (~0.9, ~0.1, 1/4) site was attributed solely to Na3. Refinement of the Li⁺ ions was complicated by the strong correlation between occupation and thermal parameters; an isotropic displacement parameter was thus used for Li4, while the other Li⁺ ions were refined with anisotropic displacement parameters. These correlations lead to large standard deviations for the displacement parameters of the Li⁺ ions (Table 2, *i.e.* Li1).

The extra oxygen, O6, involved in the Frenkel defect is included in the model as a fixed contribution at the mO site (5/6, 1/6, 1/4) and given an isotropic displacement parameter. Its occupation (~11%) was checked in a preliminary refinement. The associated Al atom, Al5, is refined at $z \simeq 0.175$ (Fig. 2*b*) with an occupation corresponding to that of O6. The occupation of Al1 is decreased by a corresponding amount.

Anisotropic displacement parameters were refined for all atoms, except Li4 and O6; all refined parameters are given in Table 2.
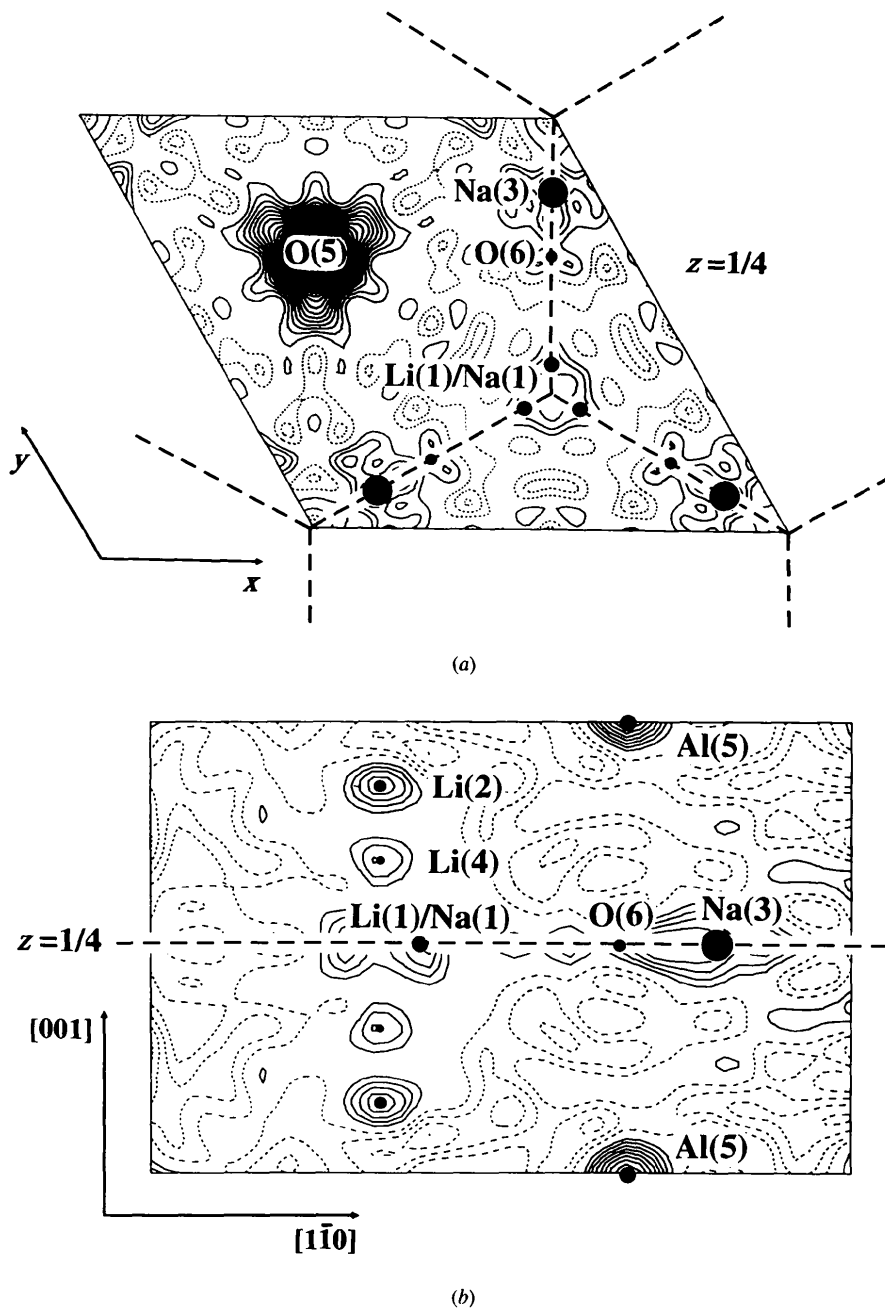

(*a*)

(*b*)

Fig. 2. Observed Fourier synthesis at 298 K for Li⁺/Na⁺ β-alumina in (*a*) the conduction plane at $z = 1/4$, contour intervals 0.5 e Å⁻³; (*b*) the $(x,-x,z)$ plane, contour intervals 0.2 e Å⁻³.

Table 2. *Fractional atomic coordinates and equivalent isotropic displacement parameters* ($\mathring{A}^2$)

$$U_{eq} = (1/3)\Sigma_i\Sigma_j U^{ij}a_i^*a_j^*\mathbf{a}_i.\mathbf{a}_j.$$

	Site	f.o.*	x	y	z	U_{eq}
X-ray, 30 K						
Al1	12(k)	0.963†	−0.167876 (18)	−0.33575 (4)	0.105381 (9)	0.00417 (8)
Al2	4(f)	1	1/3	2/3	0.024598 (14)	0.00292 (8)
Al3	4(f)	1	1/3	2/3	0.175518 (14)	0.00604 (9)
Al4	2(a)	1	0.0000	0.0000	0.0000	0.00317 (11)
O1	12(k)	1	0.15703 (4)	0.31406 (7)	0.049758 (18)	0.00441 (12)
O2	12(k)	1	0.50299 (4)	−0.50299 (4)	0.145923 (19)	0.00588 (10)
O3	4(f)	1	2/3	1/3	0.05520 (3)	0.00422 (16)
O4	4(e)	1	0.0000	0.0000	0.14148 (3)	0.00389 (16)
O5	6(h)	0.333	0.312 (2)	0.688 (2)	1/4	0.051 (4)
Al5	12(k)	0.037†	−0.1601 (5)	−0.3202 (9)	0.1762 (2)	0.00417 (8)
Li2	4(f)	0.142 (6)	2/3	1/3	0.2043 (7)	0.006 (4)
Na3	6(h)	0.421 (8)	0.9058 (9)	0.0942 (9)	1/4	0.065 (6)
Li1	6(h)	0.156 (9)	0.7032 (13)	0.2968 (13)	1/4	0.023 (5)
Na1	6(h)	0.016†	0.7032 (13)	0.2968 (13)	1/4	0.023 (5)
O6	6(h)	0.037†	0.8333	0.1667	1/4	0.0380
X-ray, 298 K						
Al1	12(k)	0.963†	−0.167959 (11)	−0.33592 (2)	0.105473 (9)	0.00570 (5)
Al2	4(f)	1	1/3	2/3	0.024607 (13)	0.00416 (6)
Al3	4(f)	1	1/3	2/3	0.175609 (13)	0.00750 (7)
Al4	2(a)	1	0.0000	0.0000	0.0000	0.00444 (8)
O1	12(k)	1	0.15713 (2)	0.31426 (5)	0.049761 (12)	0.00575 (8)
O2	12(k)	1	0.50294 (3)	−0.50294 (3)	0.146040 (13)	0.00752 (10)
O3	4(f)	1	2/3	1/3	0.05525 (2)	0.00559 (11)
O4	4(e)	1	0.0000	0.0000	0.141512 (19)	0.00518 (13)
O5	6(h)	0.333	0.3051 (8)	0.6949 (8)	1/4	0.049 (2)
Al5	12(k)	0.037†	−0.1595 (4)	−0.3190 (9)	0.1764 (2)	0.00570 (5)
Li2	4(f)	0.128†	2/3	1/3	0.2043 (7)	0.014 (4)
Na3	6(h)	0.421 (8)	0.9093 (6)	0.0907 (6)	1/4	0.072 (4)
Li1	6(h)	0.156†	0.6994 (15)	0.3006 (15)	1/4	0.040 (6)
Na1	6(h)	0.016†	0.6994 (15)	0.3006 (15)	1/4	0.040 (6)
O6	6(h)	0.037†	0.8333	0.1667	1/4	0.0253
Li4	4(f)	0.014†	2/3	1/3	0.2271	0.0443

* The fractional occupation (f.o.) given here does not include the site multiplicity correction factor, *i.e.* a fully occupied site is always given as the fractional occupation 1.0.   † Fixed value.

Refinement of the column O5 atom stabilized when it was shifted from a 2(c) site to a disordered 6(h) site (Table 2). The neutron diffraction study also showed O5 to be disordered.

The final X-ray model was then tested on the neutron diffraction data. A scale factor and all the spinel-block atom parameters were refined, with the Li$^+$ and Na$^+$ ion parameters fixed to their X-ray determined values. The resulting Fourier difference map for the conduction plane (Fig. 4) showed that the model taken from the X-ray experiment fitted well to the neutron diffraction data, even if the distribution of scattering power around the BR site was not described perfectly.

The symmetry of the majority of the structure (the spinel-block host) is here imposed onto a minority component (the mobile ions), which cannot reasonably share this same symmetry at a local level. A lower symmetry model for the mobile ions was thus tested by the removal of the mirror operation for the ions in the conduction plane through the use of the space group $P6_3mc$. The result did not improve, however.

3.2. Structure at 30 K

The low-temperature X-ray study (30 K) was made in an attempt to better resolve the content of the conduction

plane. The anisotropic displacement parameters for the atoms in the spinel block were lower than in the room-temperature structure, while the values for the ions in the conduction plane were roughly the same at both temperatures (Table 2). These parameters thus describe the distribution of the ions in their conduction pathways rather than their vibrational properties. The disorder in O5 persists at 30 K (see the unusually high displacement parameter in Table 2). The Na$^+$ ions refined to almost the same occupational and positional parameters as at 298 K (Table 2). The significant difference between the structures at 30 and 298 K lay in the distribution of the Li$^+$ ions. At 30 K, the Li$^+$ ions were found at (~0.70, ~0.30, 1/4) and (2/3, 1/3, 0.204). The (2/3, 1/3, 0.227) site was not occupied (Fig. 3).

4. Discussion

The structure comprises Al atoms octahedrally and tetrahedrally coordinated by O atoms to form spinel layers separated in the c direction by Al3—O5—Al3 bridging bonds (Fig. 1). The 'conduction planes' (at $z = 1/4$ and $z = 3/4$) only contain the column O5 atoms, the mobile Li$^+$ and Na$^+$ ions, and (in roughly 11% of the unit cells) the extra O6 atoms. The Li$^+$ ions are distributed along

edge-linked hexagonal pathways around the O5 atoms. The BR and aBR sites [aBR = anti-Beevers–Ross site, a 2(b) site at (0, 0, 1/4)] constitute the junctions in the conduction pathways, with the space available at BR sites somewhat greater than at aBR sites, favouring occupation by Li⁺ or Na⁺ ions. Indeed, the Li⁺ ions are found at sites near the BR site, here denoted as Li1, Li2 and Li4. The Na⁺ ions are found at the Li1 site and at a site denoted Na3; the aBR sites are essentially empty. In Na⁺ β-alumina, the O5 atom occupies a 2(c) site. In this present structure the O5 atom is disordered and

shifted from the 2(c) to a 6(h) site. The extra O atoms occupy mO sites [mid-oxygen site, a 6(h) site at (5/6, 1/6, 1/4)], and are bonded to the spinel block via interstitial aluminium ions, Al5, at $z = 0.175$ and $z = 0.325$. These have become displaced from the Al1 site (see Fig. 1). This Frenkel defect (Roth, Reidinger & LaPlaca, 1976; Reidinger, 1979) can be seen to have a negative effect on ionic mobility in that it effectively blocks some of the pathways in forming a local structural unit involving its nearest positive ions (Edström, Thomas & Farrington, 1991a,b).
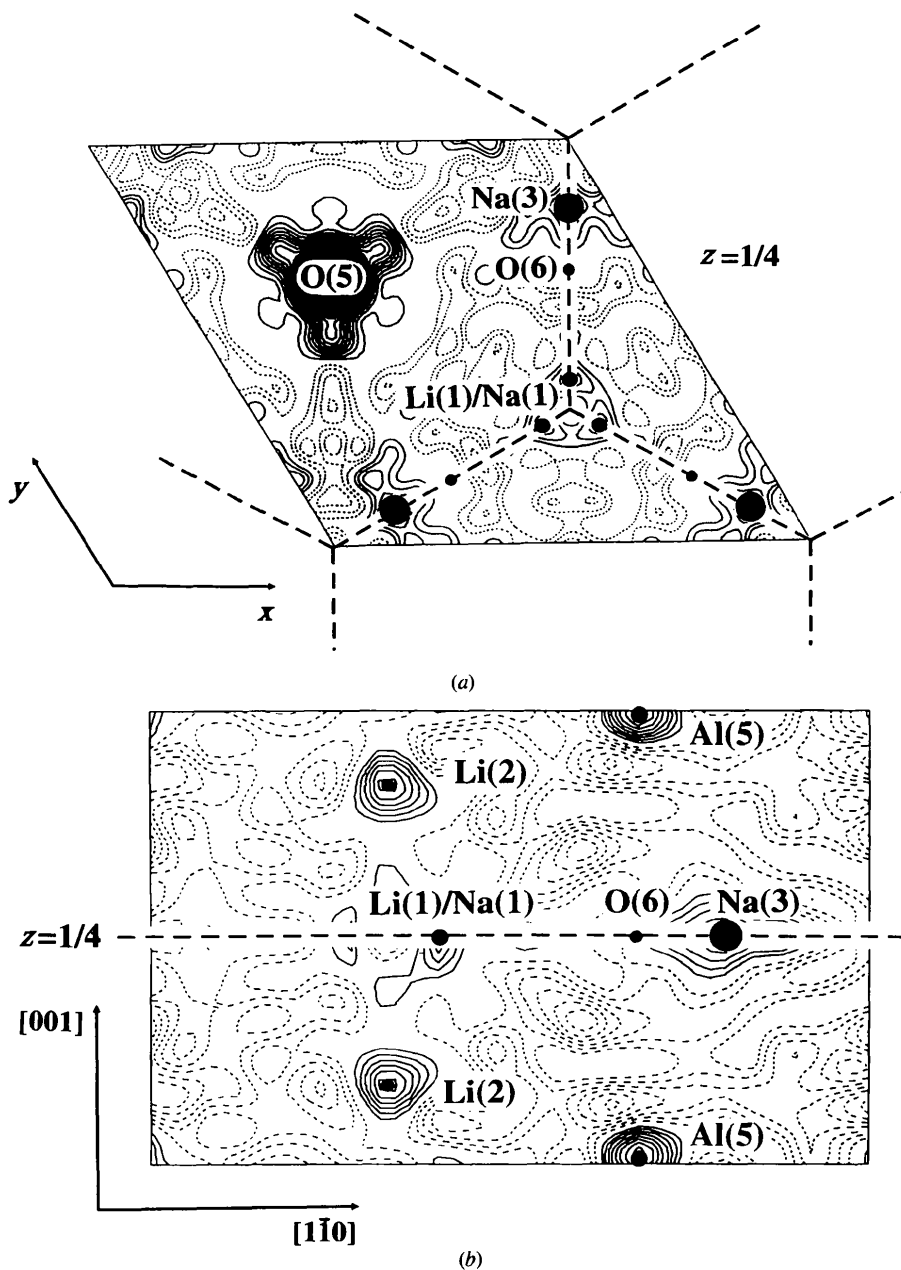

(a)

(b)

Fig. 3. Observed Fourier synthesis at 30 K for Li⁺/Na⁺ β-alumina in (a) the conduction plane at $z = 1/4$, contour intervals 0.5 e Å⁻³; (b) the $(x,-x,z)$ plane, contour intervals 0.2 e Å⁻³.
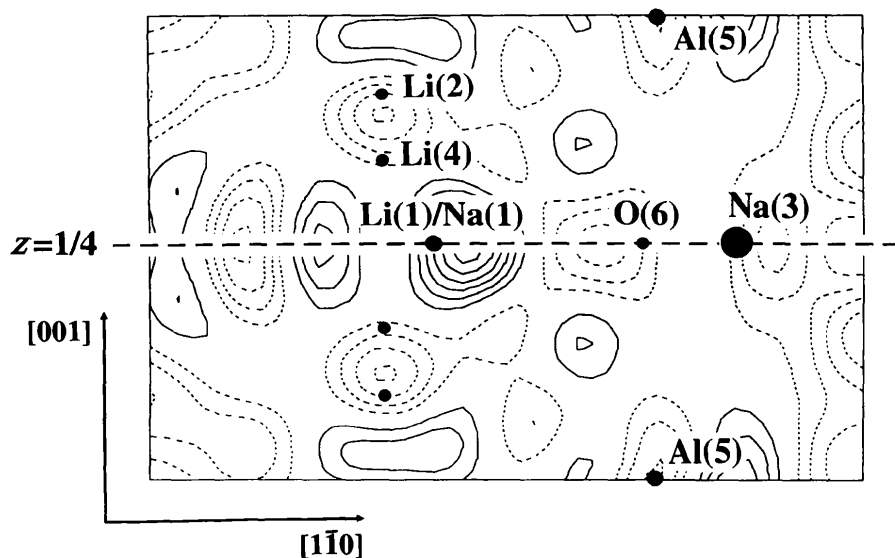
Fig. 4. Difference-Fourier synthesis for neutron diffraction of Li^+/Na^+ β-alumina in the $(x,-x,z)$ plane, where the model describing the ionic distribution is taken from X-ray diffraction at 298 K. Contour interval 0.02 e $Å^{-3}$.

The structural result from this present study must be related to the structure of the mother compound Na^+ β-alumina, which has the same general structure as Li^+/Na^+ β-alumina, with rigid spinel blocks of aluminium oxide and conduction planes, hosting the Na^+ ions: 0.73 Na^+ is in BR sites and 0.49 Na^+ in A-type sites, a 6(h) site noted A at the position ($\sim$0.9, $\sim$0.1, 1/4) (Edström, Thomas & Farrington, 1991a,b). The reason for this Na^+ ion distribution and its impact on the conductivity mechanism has been discussed earlier by several different authors (Edström, Thomas & Farrington, 1991b; Roth, Reidinger & LaPlaca, 1976; Reidinger, 1979; Zendejas & Thomas, 1990). It would now seem clear that the Frenkel defect is intimately responsible for the mobile-ion distribution. The Na^+ ions in the A site are trapped by the O6 atom and a local structurization of the Na^+ ions around the O6 atom (Fig. 5).

When the Li^+ ions begin to exchange with the Na^+ ions, the Na^+ ions at the BR site seem to be the first to be exchanged. The combination of X-ray (Figs. 2 and
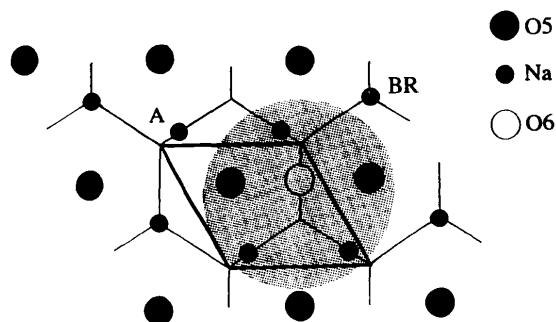

Fig. 5. Sphere of greatest influence around O6, the charge compensating O atom, in β-alumina.

3) and neutron diffraction suggests that the majority of the electron density and the scattering power comes from Li^+ ions in this site. Not only are almost all the Na^+ ions replaced in this site, but the Li^+ ions also occupy a new site at 30 K and two new sites at 298 K. These sites are closer to the O atoms of the spinel block, with the Li—O distances $\sim$2.0 Å (see Table 3). The c axis of the present compound, 22.652 (3) Å, is also significantly longer than for pure Na^+ β-alumina, 22.526 (3) Å (Edström, Thomas & Farrington, 1991a,b); see also Table 1. In the neutron diffraction study the scattering amplitude is positive at the site at $\sim$0.91, $\sim$0.09, 1/4, which means it is probably occupied by Na^+ ions. The combination of the X-ray with the neutron diffraction result confirm this. This contrasts with the mixed-ion system Na^+/Cd^{2+} β-alumina (Edström, Thomas & Farrington, 1991b), where the Na^+ ions at ($\sim$0.91, $\sim$0.09, 1/4) were the first to be exchanged. This was attributed to the strong coulombic attraction between the extra O6 atom, and the Na^+ and Cd^{2+} ions, respectively. Also in this present case the results can be interpreted in terms of a cluster of Na^+ ions in which the Na^+ ions found in the ($\sim$0.91, $\sim$0.09, 1/4) site, corresponding to the A site in Na^+ β-alumina, do not exchange in a lithium salt melt, due to Na—O6 attraction forces. These would seem to remain in the structure after the majority of the Na^+ ions in the BR site have been exchanged for Li^+ ions. It has been found earlier in polycrystalline samples that it is difficult to exchange more than $\sim$60% of the Na^+ ions (Tofield & Farrington, 1979).

We see then that the Li^+ ion is unique in its behaviour as a monovalent ion in the β-alumina host. No other ion has been found to reside well outside the mirror plane (at z = 1/4 and 3/4). This can imply a different conductivity mechanism for Li^+ ions than for any other ion-type in β-alumina. The mean ion distribution at the

Table 3. *Selected geometric parameters (Å, °) from X-ray studies*

	30 K	298 K
Al1—O1 × 2	2.0175 (3)	2.0200 (2)
Al1—O2 × 2	1.8392 (3)	1.8400 (2)
Al1—O3 × 1	1.9644 (4)	1.9648 (3)
Al1—O4 × 1	1.8196 (3)	1.8200 (2)
Al1—Al5 × 1	1.607 (5)	1.609 (5)
Al2—O1 × 3	1.7996 (4)	1.7995 (3)
Al2—O3 × 1	1.8079 (8)	1.8089 (5)
Al3—O2 × 3	1.7742 (3)	1.7743 (2)
Al3—O5 × 3	1.6998 (13)	1.7072 (7)
Al4—O1 × 6	1.8927 (4)	1.8941 (2)
Al5—O2 × 2	1.772 (3)	1.776 (3)
Al5—O4 × 1	1.738 (3)	1.736 (3)
Al5—O6 × 1	1.672 (5)	1.668 (5)
Li2—O2 × 3	2.065 (10)	2.064 (10)
Li2—Li1 × 3	1.094 (14)	1.082 (15)
Li2—O6 × 3	1.917 (8)	1.918 (9)
Na3—O6 × 2	2.215 (4)	2.190 (3)
Na3—O4 × 2	2.622 (2)	2.610 (1)
Na3—O5 × 2	2.686 (11)	2.629 (5)
Na3—O5 × 2	2.938 (11)	2.973 (5)
Li1—O6 × 2	1.817 (6)	1.794 (6)
Li1—O2 × 2	2.763 (3)	2.767 (4)
Li1—O5 × 2	2.951 (12)	2.934 (8)
Li1—O2 × 4	2.763 (3)	2.766 (3)
Li1—O5 × 2	2.951 (12)	2.934 (8)
Na1—O5 × 2	2.951 (12)	2.933 (7)
Na1—O5 × 2	2.988 (12)	2.977 (7)
Li4—Li4 × 1	–	1.040*
Li4—Li1 × 3	–	0.608 (4)
Li4—Li2 × 2	–	0.517 (16)
Li4—O2 × 3	–	2.4268 (2)

* No standard deviations since the Li4 positional parameters were fixed.

room-temperature study can be interpreted in terms of a movement of Li$^+$ ions in the z direction. The Li$^+$ ions can be expected to jump back and forth between the end positions (2/3, 1/3, ~0.204) and (2/3, 1/3, ~0.227) (Fig. 3). This picture conflicts with the only other structural study by neutron powder diffraction of a mixed Li$^+$/Na$^+$ β-alumina system (Tofield & Farrington, 1979). The Li$^+$ ions were located at totally different sites on either side of the mO site (5/6, 1/6, 1/4). Despite this, the notion remains of a Li$^+$ ion diffusion mechanism involving the Li$^+$ ions hopping between sites coordinated to the oxygens of the spinel block.

5. Conclusions

We have demonstrated here the strength of combining X-ray and neutron diffraction in studying this disordered Li$^+$/Na$^+$ system. The study has provided important new information regarding conduction mechanisms for mobile ions in β-alumina. New Li$^+$ ion sites have been located lying outside the conduction plane on either side of the BR site in the β-alumina host. This structure is shown to contain a mixture of Li$^+$ and Na$^+$ ions. It can be that variable amounts of unexchanged sodium

explain the notable discrepancies in earlier conductivity measurements of what was believed to be pure Li$^+$ β-alumina. This supports an earlier suggestion of Briant & Farrington (1981). It is also clear from the present study why the last ~40% of the Na$^+$ ions can be more difficult to ion exchange in a lithium salt melt, with the Frenkel defect in the spinel block playing the decisive rôle.

References

Alpen, U. von, Bell, M. F. & Wichelhaus, W. (1978). *Electrochim. Acta*, **23**, 1395–1397.

Bates, J. B., Dudney, N. J., Brown, G. M., Wang, J. C. & Frech, R. (1982). *J. Chem. Phys.* **77**, 4838–4856.

Becker, P. & Coppens, P. (1975). *Acta Cryst.* A31, 417–425.

Beevers, C. A. & Ross, M. A. S. (1937). *Z. Kristallogr.* **97**, 59–66.

Briant, J. L. & Farrington, G. C. (1981). *J. Electrochem. Soc.* **128**, 1830–1834.

Dudney, N. J., Bates, J. B., Wang, J. C., Brown, G. M., Larson, B. C. & Engstrom, H. (1981). *Solid State Ion.* **5**, 225–228.

Edström, K., Thomas, J. O. & Farrington, G. C. (1991*a*). *Acta Cryst.* B47, 210–216.

Edström, K., Thomas, J. O. & Farrington, G. C. (1991*b*). *Acta Cryst.* B47, 635–643.

Hermansson, K. & Ojamae, L. (1993). Report UUIC-B19-475. Institute of Chemistry, University of Uppsala.

Kaneda, T., Bates, J. B. & Wang, J. C. (1978). *Solid State Commun.* **28**, 469–474.

Lehman, M. S. & Larsen, F. K. (1974). *Acta Cryst.* A30, 580–584.

Lundgren, J.-O. (1982). *Crystallographic Computer Programs*. Report UUIC-B13-04-05. Institute of Chemistry, University of Uppsala, Sweden.

McCandlish, L. E., Stout, G. H. & Andrews, L. C. (1975). *Acta Cryst.* A31, 245–249.

Radzilowski, R. H. & Kummer, J. T. (1971). *J. Electrochem. Soc.* **118**, 714–716.

Reidinger, F. (1979). Ph.D. Thesis. State University of New York, Albany, USA.

Roth, W. L., Reidinger, F. & LaPlaca, S. (1976). *Superionic Conductors*, edited by G. D. Mahan & W. L. Roth, pp. 223–241. New York: Plenum Press.

Shannon, R. D., Taylor, B. E., English, A. D. & Berzins, T. (1977). *Electrochim. Acta*, **22**, 783–796.

Sutter, P. H., Cratty, L., Saltzberg, M. & Farrington, G. C. (1983). *Solid State Ion.* **9/10**, 295–298.

Tofield, B. C. & Farrington, G. C. (1979). *Nature*, **278**, 438–439.

Yao, Y. F. & Kummer, J. T. (1967). *J. Inorg. Nucl. Chem.* **29**, 2453–2474.

Zendejas, M. A. & Thomas, J. O. (1990). *Phys. Scr.* T33, 235–244.